Moroccan Journal of Chemistry
ISSN : 2351-812X

Mor. J. Chem., 2023, Volume 11, Issue 01, Page 188-204
https://revues.imist.ma/index.php/morjchem

Assessment of the Corrosion Inhibitory Potentials of *Chromolaena Odorata* Leaf Extract on Mild Steel in Hydrogen Chloride Acid Environment

Ezeh Ernest Mbamalu[1] and Agu Peter Chinedu[2]

[1]*Department of Chemical Engineering, Caritas University, Amorji Nike Enugu Nigeria*
[2]*Department of Science Laboratory Technology (Biochemistry), Osisatech Polytechnic, Enugu Nigeria*
** Corresponding author Ezeh, Ernest Mbamalu. Email- mbamalu06@gmail.com*

Received *11 Feb 2022,*
Revised *15 Jan 2023,*
Accepted *19 Jan 2023*

Citation*: Ezeh E. M., Chinedu Agu P.., (2023) Assessment of The Corrosion Inhibitory Potentials of Chromolaena Odorat Leaf Extract On Mild Steel In Hydrogen Chloride Acid Environment, Mor. J. Chem 14(1), 188-204. Doi: https://doi.org/10.48317/IMIST.PRSM/morjchem-v10i3.30521*

Abstract This study aims to evaluate the corrosion inhibitory potential of *Chromolaena Odorata* leaf extract (*COL*) on mild steel in a hydrogen Chloride acid (HCl) medium. A gravimetric method was used for the corrosion control experiment. The inhibition efficiency was optimized using the responses surface methodology. The protective film formed on the mild steel surface was analyzed by Fourier Transmission Infrared (FTIR) spectroscopy and Scanning Electron Microscopy (SEM). The electrochemical parameters of the corrosion test were investigated, the corrosion rate progressively decreased with time, with a maximum inhibition efficiency of 83.33%, whereas the corrosion rate reduced from 17.79 to 3.704mgcm^{-2}h^{-1}. FTIR analysis revealed the stretching vibrations of C≡C, C=C, C=O, and O–H bonds. The SEM images show that the addition of *COL* inhibitor remarkably decreased the rate of mild steel corrosion. This study showed that *COL* plant extracts effectively inhibited mild steel corrosion in 1M HCl. *COL* plant extract. Therefore, it served as an eco-friendly and effective green corrosion inhibitor for mild steel in an acidic medium

Keywords: Corrosion rate; Inhibition efficiency; *Chromolaena Odorata*; FTIR analysis; SEM image; Optimization.

1. Introduction

Metals are widely used in human activities due to their excellent mechanical and electrical properties (Ashmawy & Mostfa, 2021). To preserve the desired state of these metals, their corrosion maintenance and control are vital. Corrosion is probably the most common undesired phenomenon that makes metals become weaker (Sulaiman et al., 2019). This natural process originates from the electrochemical interaction of metals with the corrosive environment. Sulfides, oxides, and

others are generated through reactions between the metal surface and the corrosive medium (Guruprasad et al., 2020).

Among metals, mild steel is the most widely used in the oil, food, energy, chemical, and construction industries due to its wide applications, most of which are consequent on its excellent mechanical properties (Rostampour et al., 2020). This metal shows high mechanical resistance, durability, and toughness, among other, applications, which makes it a highly available material and at a relatively low cost. Consequently, solutions to problems relating to degradation by the corrosion of mild steel are a priority subject. The high cost associated with corrosion, due to the replacement of corroded metals, could be mitigated by the application of corrosion inhibitors (Rocca et al., 2019; Umoren et al., 2016)

Constituting the perfect source for mineralization and corrosion phenomena, seawater is an example of a common corrosive medium, containing an abundance of chloride ions, including massive water bodies around the world: oceans, seas, and salt lakes (Farssi et al., 2020; Zheng et al., 2021) On the other hand, hydrochloric acid (HCl) is frequently used both in decalcification processes and to produce corrosion under controlled conditions (Mechbal et al., 2016). Several authors employ 1M HCl solutions, making it the most prominent corrosion medium to study corrosion since it is extremely aggressive and can be used to obtain an idea regarding corrosion on a certain metal. Other solutions recurrently used as corrosive media are 3.5% NaCl, 0.1 M HCl (Bouayad et al., 2017) and 0.1 M NaOH. To a lesser extent, 1M H_3PO_4 and 0.5 M H_2SO_4 are used as test solutions as well (Aoufir et al., 2017).

Corrosion inhibitors are substances that are added in small amounts on metal surfaces or are added to the corrosive medium, reducing the tendency to be affected by corrosion. The use of common corrosion inhibitors is sometimes limited since these are based on dangerous substances for human health, such as chromium-based treatments (Sabbahi et al., 2020). Recent approaches take advantage of organic compounds that can be obtained from expired pharmaceutic drugs, mushroom extracts, and even plant extracts (Hashim et al., 2019; Jing et al., 2021). There is a variety of green organic compounds that function as corrosion inhibitors that show excellent properties in protecting metal surfaces, for example, derivatives of chitosan phenylmethanimine, imidazoline, and ionic liquid (Lou et al., 2021). In consequence, these compounds replace the traditional toxic corrosion inhibitors. Highly efficient corrosion inhibitors have been achieved utilizing these substances, providing new recycling and reusing routes for drugs as well as corrosion inhibitors obtained from sustainable, ecological, and environmentally friendly sources, with plant extracts being a prominent group (Begum et al., 2021; Guo et al., 2020). These extracts constitute another option of great interest since they offer the possibility of a first approach to determine the classes of natural compounds that help inhibit the corrosion process. The advantage is that making an extract from any plant is regarded as an uncomplicated task, thus allowing more efficiency at both extraction and use of these substances for experimentation.

An extract is a solution composed of the active principles of a plant or its parts and a certain medium acting as a solvent. The extraction yields depend on the polarity of the solvent used, in the techniques or methods (Soxhlet and maceration), among others. Active principles contained in the extract give the properties for a particular purpose. Thus, a given plant, in terms of its active principles and concentrations, can be associated with some benefits. These extracts are mostly known for their antioxidant, anti-inflammatory, antiviral, or antimicrobial effects. In addition, their corrosion inhibitor properties can be considered synergic effects(Yan et al., 2019). Extracts are commonly obtained from the whole plant or the parts containing higher concentrations of active principles, named

phytochemicals (Begum et al., 2021). According to the literature, extracts of plants, fruits, seeds, flowers, and leaves contain active compounds that are promising for corrosion inhibition in aggressive media. Moreover, these compounds become cheap, widely available, and renewable corrosion inhibitor alternatives (Denissen & Garcia, 2019)

Extensive work on corrosion control by inhibition has covered areas such as microbial inhibition, chemical inhibition, petrochemical inhibition, and other artificial forms of inhibition. Although these micro acids are effective inhibition measures, they have adverse effects, for example, lead compounds present in paint formulations are well known for their toxic carcinogenic effect, and other corrosion inhibitors such as benzene nitrates and phosphorus, exhibit toxic and adverse environmental effects (Zinad et al., 2020). However, the need to develop effective environmentally friendly features is the common jingle in science today (Fateh et al., 2020) . In this regard, many researchers have embarked on the use of an organic inhibitor of plant sources to prevent corrosion of metals, of which their research results proved effective and efficient. The expanded interest in organic inhibitors of plant sources otherwise called green inhibitors is attributed to the fact that they are cheap, ecologically friendly, and pose no environmental threat, and the fact that they are readily available, renewable sources of material, ls and sustainable the corrosion inhibition properties in many plant extracts are due to their heterocyclic constituents like alkaloids, flavonoids, tannins, etc. Again, it is suggested that medicinal plants possess good corrosion inhibition properties since they are constituted of compounds containing hetero-atoms like N, S, O, and P which are reported to have corrosion inhibiting properties (Wood & Clarke, 2017) The above reasons lead to our interest in *COL* leaves. Its abundant organic components in which N, S, and O atoms are the constituent atoms (Song et al., 2021). However, it has never been studied in acid solutions for corrosion inhibition. To explore this possibility, an attempt has been made to ascertain its corrosion inhibition potentials. In this present work, the corrosion inhibiting properties of the extract of *COL* in 1 M HCl were studied using weight loss and electrochemical methods. The study though is limited to the use of mild steel, but it is presumed that findings may apply to other metals/alloys since most industries make use of similar metals and alloys and there is usually a high chance of exposing them to a similar corrosion environment (Ogunleye et al., 2020)

2. Methodology

2.1 Mild Steel Preparation

The mild steel used for this study was cut into corrosion coupons of size 1 cm × 2.5 cm × 0.05 cm. The surface preparation of the mechanically polished specimens was carried out using different grades of emery paper and then degreased with acetone after washing with distilled water.

2.2 Preparation of *COL* Leaf Extract

The leaves of *COL* were obtained from a local garden in Obiofu Nenwe Aninri Local Government Area, Enugu State, Nigeria. They were identified in the Department of Botany, University of Nigeria Nsukka. The leaves were dried in an N53 C-Genlab laboratory oven at 60^{o}C and size reduced to powder form in an electric grinding machine. 50 g of the powder was extracted continually with 250 cm^3 of absolute ethanol in a Soxhlet extractor for 24 hours. The extract was heated in a water bath at 50^{o}C until almost all of the ethanol evaporated to form a gel. 12 g of the gel was dissolved in 500 mL of 5.0 M H_2SO_4 solution, agitated vigorously, and kept overnight (24 hours). The resultant solution was filtered and stored. This stock solution (24 g/L) was used to prepare test solutions of different concentrations of the inhibitor; 0.1, 0.3, 0.5, 0.,7, and 0.9 g/L. The test solutions for the inhibitor were prepared by serial dilution of the stock solution.

2.3 Weight loss method

Mild Steel specimens of size 1 cm × 2.5 cm × 0.05 cm were used in weight loss experiments. Mild steel composed of (wt %) Fe 99.30%, C 0.076%, Si 0.026%, Mn 0.192%, P 0.012%, Cr 0.050%, and Ni 0.050% were pre-treated before the experiment by grinding with emery paper (grade 600, 800, 1000 and 1200) then cleaned with double distilled water, degreased with acetone and dried. After weighing accurately using a digital balance with a sensitivity of ±0.01 mg, the specimens were immersed in 250 ml test solutions (Onyeka et al., 2020). All the aggressive acid solutions were open to the air. The measurements were performed at 30 ℃ (except for temperature effect) for 3h (except for immersion time effect) without and with various amounts of inhibitors. After the elapsed time, the specimen was taken out, washed, dried,d, and weighed accurately. All the tests were conducted in aerated 1 M HCl. All the experiments were performed in triplicate and average values were recorded. The concentration of inhibitor for weight loss and the electrochemical study was taken in mg L^{-1}

The weight loss (Δw), corrosion rate (CR), and inhibition efficiency (IE) were calculated using the Equations (1), (2,) and (3) respectively:

$$\Delta w = w_i - w_f \quad (1)$$

$$CR = \frac{w_i - w_f}{At} \quad (2)$$

$$IE\% = \frac{\omega_0 - \omega_1}{\omega_0} x100 \quad (3)$$

Where w_i and w_f are the initial and final weight of mild steel samples respectively; ω_1 and ω_0 are the weight loss values in the presence and absence of *COL* leaf extract (inhibitor), respectively. A is the total area of the mild steel sample and t is the time of immersion.

2.4 Electrochemical Analysis

The electrochemical studies were performed by using a three-electrode cell (Plate1). The cell consisted of mild steel as the working, a silver chloride (Ag/AgCl) as the reference, and a platinum sheet (with a 1 cm^2 surface area) as the counter electrode. A cylindrical rod of mild steel in a polyester block with an exposed surface of 0.2 cm^2 was used. The chemical composition (wt. %) of the mild steel was given in Table 1. Before each measurement, the working electrode was polished with 400, 800and, 1200 grades of emery papers and washed in distilled water. All electrochemical measurements were made with a computer-controlled electrochemical analyzer Gamry ZRA. The surface characterizations of the electrodes were done using SEM (Zeiss /Supra) and FT-IR (Perkin Elmer, Frontier) instruments. Infrared spectra were recorded in the wave number range of 400-4000 cm^{-1}.

2.5 Phytochemical Analyses of *COL* leaf extract.

2.5.1 Qualitative analyses of the sample

For the alkaloid detection, 1g of solvent-free leaf extract was transferred in to test tube. A few drops of dilute hydrochloric acid were added and stirred. It was then filtered. The filtrate was tested carefully with alkaloid reagents; Mayer's reagent (Cream ppt), and GrSagendorf'sff's reagent (Orange-brown ppt). In the detection of cardiac glycosides, 1ml of the sample, 5ml water, and 2ml glacial acetic acid were mixed in a vessel. One drop of $FeCl_3$ was added. Then, 1ml conc. H_2SO_4 was added. There was an appearance of a brown ring. For the determination of flavonoids, 25 ml water was added to 1g of

sample. It was put in an oven at 100°C for 15 min. 5ml of NH_4OH was added to 2ml of the sample.(O.D & Ezeh, 2021) Then 1ml conc. H_2SO_4 was added. There was an appearance of yellow colour indicating the presence of flavonoids. The presence of phenols was determined by adding a few drops of 1% (w/v) solution of ferric chloride followed by 1% (w/v) gelatin in sodium chloride of the same concentration. The formation of a precipitate indicated the presence of phenols. For the determination of saponins, 1g of sample was boiled in 40ml of water and then filtered. 10ml of the filtrate was shaken vigorously. The formation of froth was noticed. 3 drops of oil were added, and the mixture was shaken. Emulsion of the oil was noticed. For the determination of tannins, 1g of the sample was added to 25ml of water. It was then put in the oven at 100°C for 15 min. To 1ml of the sample, 10ml water was added and then boiled. A few drops of 0.1% $FeCl_3$ were added. A green colour appeared indicating the presence of tannins.

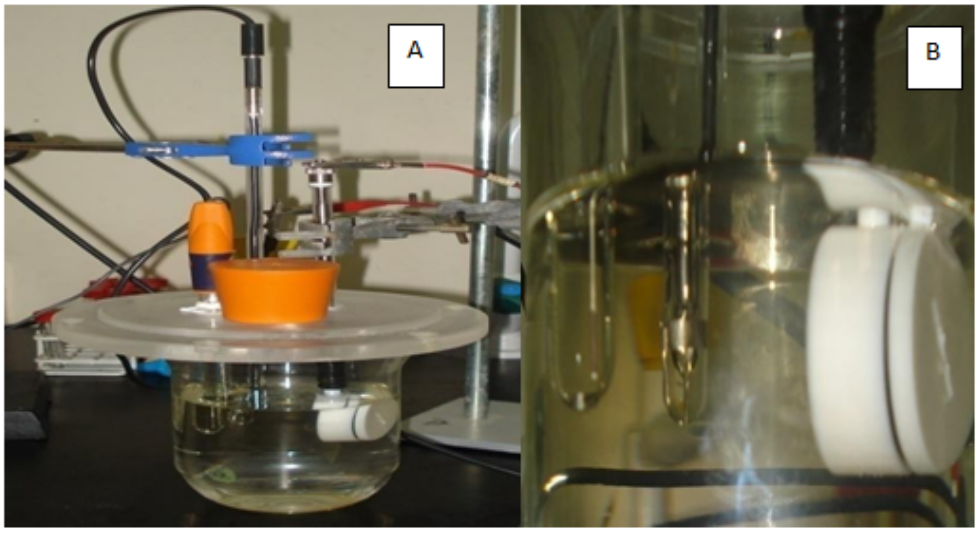

Plates 1A and 1B: (1A) Electrochemical cell used in the electrochemical analysis. (1B) Three used electrodes: Reference, Auxiliary, and the Teflon working electrode.

2.5.2 Quantitative analyses of the sample

a. Alkaloids

20ml of 10% acetic acid in ethanol was added to the 1g of sample. The mixture was shaken and allowed to settle for 4 hours. It was then filtered. The filtrate was evaporated to about a quarter of its original volume. One drop of concentrated ammonium hydroxide was added. The precipitate formed was filtered through a weighed filter paper. The filter paper was left to dry in the oven at 60°C. The filter paper was weighed after drying it to a constant weight.

$$t Alkaloid = \left(\frac{w_r - w_f}{w_0}\right) \quad (4)$$

Where w_r is the weight of filter paper + residue, w_f is the weight of filter paper, and w_0 is the weight of the sample analyzed.

b. Cardiac glycosides

1g of the sample was placed in the oven 100 ^{0}C for 15min. 1ml of the sample plus 5ml water was added to 2ml glacial acetic acid plus one drop of $FeCl_3$. Also, 1ml conc. H_2S0_4 was added. The absorbance of the resulting solution was measured at 410nm.

c. Flavonoids

0.5ml of 2% $AlCl_3$ methanol solution was added to 0.05ml sample solution. After 1hr at room temperature. A yellow colour appeared indicating the presence of flavonoids. Flavonoids content as mg/g quercetin was determined.

d. Phenols

0.2% formic acid was added to 2g of the sample and left to settle for 2 minutes. It was then filtered. With the aid of a pipette, 2ml of the filtrate was put into a test tube and 0.5ml folin-Cocteau reagent was added. It was left for 20 minutes for colour development. The absorbance at 765nm was read and the concentration for a standard graph was obtained. It is expressed as GAE/g (Gallic Acid Equivalent) (Ezeh et al., 2019).

e. Phytate

Ferric ammonium sulphate was added to 0.5ml of the sample in a test tube. The test tube was heated in a water bath for 30 minutes. It was cooled and centrifuged. To 1ml of the supernatant, 1.5 ml of 2, 2-bipyridine solution was added. Measurement was carried out at 519nm, with distilled water as blank.

f. Saponins

Into 1g of sample 15 ml, ethanol was added and put in a water bath at 55^{o}C for 4 hours. It was filtered and the residue was washed twice with 20% ethanol. The sample was reduced to about 5 ml in the oven. 5ml of petroleum ether was added to the concentrated sample inside a separating funnel. The petroleum ether layer was discarded and 3ml of butanol was added to it. It was washed with 5ml of 5% sodium chloride. It was put in the oven to evaporate to dryness, and the residue was weighed (Aniobi et al., 2021).

g. Tannins

1g of the sample was extracted with 25ml of the solvent mixture of 80: 20 acetones: 10% glacial acetic acid for 5 hours. It was filtered and the absorbance was measured at 500nm. The absorbance of the reagents blank was also measured. A standard graph with 10, 20, 30, 40, and 50 mg/100g of tannic acid was drawn. The concentration of tannin (taking into consideration any dilution factor) was obtained.

2.6 Determination of the Effects of Corrosion parameters

Effects of corrosion parameter variables: inhibitor concentration, temperature and time on weight loss, corrosion rate and inhibition efficiency were determined. The weight-loss method was applied as the independent variables were varied in the experimental runs with the dependent variable. The results of each run are expressed in tables 3,4 and 5.

2.7 Scanning Electron Microscopic Study

The morphology of corrosion of mild steel was analyzed using a scanning electron microscope (SEM) Plate 2. Scanning electron microscopy (SEM) measurements were carried out using an FEI Quanta 200 (FEI Co., Eindhoven, the Netherlands) electron microscope and operated at an accelerating voltage of 20/10 kV. Test samples were prepared by freezing them in liquid nitrogen before fracturing to expose the cross-sectional area for visibility of the test samples' distribution and morphology (Ezeh & Onukwuli, 2021).

2.8 Optimization of the inhibition efficiency

On the response surface methodology (RSM), Design-Expert software was used to design the experiment. Interactive effects of inhibitor concentration, temperature and time on the inhibition efficiency were determined. The design matrix is shown in Table 1.

Plate 2: Photograph of Scanning Electron Microscope (SEM) Instrument (Ezeh & Onukwuli, 2020)

Table 1: Experimental Design Matrix

Std	Run	Factor 1 An Inhibitor conc. g/L	Factor 2 B Temperature K	Factor 3 C Time hr	Response Inhibition efficiency %
5	1	0.5	303	5	
4	2	0.9	323	1	
14	3	0.7	313	5	
3	4	0.5	323	1	
13	5	0.7	313	1	
7	6	0.5	323	5	
8	7	0.9	323	5	
10	8	0.9	313	3	
17	9	0.7	313	3	
12	10	0.7	323	3	
19	11	0.7	313	3	
11	12	0.7	303	3	
20	13	0.7	313	3	
1	14	0.5	303	1	
2	15	0.9	303	1	
6	16	0.9	303	5	
9	17	0.5	313	3	
16	18	0.7	313	3	
15	19	0.7	313	3	
18	20	0.7	313	3	

3. Results and Discussion

3.1 The Qualitative and Quantitative Results of the Phytochemicals

The qualitative results of the phytochemicals are denoted with symbols; +++ (highly concentrated), ++ (concentrated), + (in traces), and – (absent or too little to be observed qualitatively) (Table 2). These phytochemicals are commonly found in plants and their presence in the phytochemicals showed that *COL* leaf extract is a suitable corrosion inhibitor (Edoziuno et al., 2020).

Table 2: Qualitative and Quantitative Analysis of *COL* leaf extract

Phytochemicals	Qualitative analysis	Quantitative analysis
Alkaloids (mg/100g)	+++	277.5
Cardiac glycosides (mg/100g)	+	38.1
Flavonoids (mg/100g)	-	10.6
Phenolics (GAE/g)	++	102.3
Phytates (mg/100g)	+	55.0
Saponins (mg/100g)	++	144.7
Tannins (mg/100g)	+++	251.4

3.2 Effects of Process Variables on the Efficiency of *COL* Leaf Extract Inhibitor

Effect of process variables of time, inhibitor concentration and temperature on the corrosion control are shown in tables 3, 4 and 5 respectively. The weight loss, corrosion rate, inhibition efficiency and degree of surface coverage were obtained at 0.7 g/L inhibitor concentration, 30°C and 3hrs time of immersion. The inhibition efficiency was obtained as a function of inhibitor concentration, temperature and time. In all of the cases, inhibition efficiency increased with an increase in all of the process variables till it got to the peak. The degree of surface coverage is directly related to the inhibition efficiency. Both of them are used for measuring the effectiveness of corrosion inhibitors.

For process variable time, it was observed that an increase in time increased inhibition efficiency until it got to the peak at time 3hrs from where a decrease in the inhibition efficiency was noticed from 83.33 % at time 3hrs to 82.95% and down to 79.72 %. The maximum inhibition efficiency of 83.33 % was obtained at the time 3hrs. Also, an increase in temperature increased inhibition efficiency until it got to the peak at temperature 313 k from where it started to decrease. The maximum inhibition efficiency of 83.33 % was observed at a temperature of 313 k. Similarly, inhibition efficiency increased with an increase in inhibitor concentration. This high value of inhibition efficiency showed that *COL* leaf extract is suitable for corrosion control.

Table 3: Effect of time on the corrosion control

Time (hr)	ΔW_0 (g)	CR_0 (mg/cm^{2}hr)	ΔW_1 (g)	CR_1 (mg/cm^{2}hr)	IE (%)	Θ
1	0.19	21.111	0.06	6.667	68.42	0.6842
2	0.28	15.556	0.07	3.889	75.00	0.7500
3	0.48	17.778	0.08	2.963	83.33	0.8333
4	0.5	13.889	0.11	3.056	78.00	0.7800
5	0.51	11.333	0.12	2.667	76.47	0.7647

ΔW_0 = loss in weight in the absence of inhibitor, ΔW_1 = loss in weight in the presence of inhibitor, CR_0 = corrosion rate in the absence of inhibitor, CR_1 = corrosion rate in the presence of inhibitor, Θ = degree of surface coverage, IE = Inhibition efficiency.

Table 4: Effect of inhibitor concentration on the corrosion control

Inhibitor concentration (g/L)	ΔW_0 (g)	CR_0 (mg/cm^{2}hr)	ΔW_1 (g)	CR_1 (mg/cm^{2}hr)	IE (%)	Θ
0.0	0.48	17.778				
0.1			0.22	8.148	54.17	0.5417
0.3			0.17	6.296	64.58	0.6458
0.5			0.12	4.444	75.00	0.7500
0.7			0.08	2.963	83.33	0.8333
0.9			0.1	3.704	79.17	0.7917

Table 5: Effect of temperature on the corrosion control

Temp. (K)	ΔW_0 (g)	CR_0 (mg/cm^{2}hr)	ΔW_1 (g)	CR_1 (mg/cm^{2}hr)	IE (%)	Θ
303	0.43	15.926	0.13	4.815	69.77	0.6977
313	0.48	17.778	0.08	2.963	83.33	0.8333
323	0.44	16.296	0.14	5.185	68.18	0.6818
333	0.41	15.185	0.17	6.296	58.54	0.5854
343	0.39	14.444	0.19	7.037	51.28	0.5128

3.3 FTIR analysis

Figure I show the FTIR spectrum of the protective film that adhered on the surface of mild steel coupon owing to the addition of the crushed leaves of *COL* at 0.7g per litre of 1M HCl for eight hours. The strong band at 3693.8cm^{-1} reveals the functional group of a hydrogen atom bonded to an oxygen atom (O–H stretching vibration). The strong bands at frequencies 2113.4cm^{-1}, 1871.1cm^{1}and 1636.3cm^{-1} indicated the presence of C≡C, C=O and C=C stretching vibrations of alkynes, acid anhydride and alkene respectively. CH_2 bending was also spotted around 1461.1cm^{-1}.

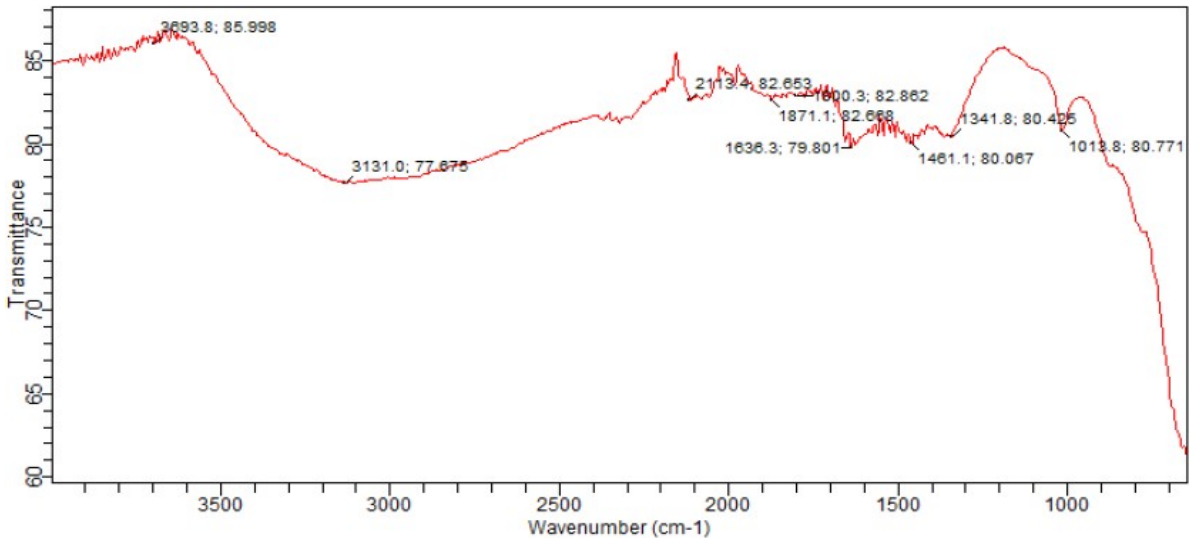

Figure I: FTIR spectrum of film on mild steel surface after Immersion for three hours in a medium containing the thoroughly crushed fresh leaves of *COL* at 0.7g per litre of 1M HCl

3.4 SEM micrograph for the corrosion inhibition of mild steel in 1 M HCl solution by the crushed leaves of *COL*

Plate 3A and 3B show the SEM image of the corrosion of mild steel in an uninhibited solution of 1M HCl. Corrosion was observed not to take place identically over the surface of the steel. However, the addition of the crushed leaves of COL at 0.7g per litre of 1M HCl protected the surface of the steel from corrosion as shown in Plate 3B in comparison with the inhibitor-free solution Morphological Examination Plate3A. Scanning electron microscopy was used to analyze the textural properties of the coupons in the unprotected and protected environment at magnifications of 1500×179 µm and 350×766 µm, respectively. Figure 4A revealed the mild steel after 21 h of immersion in blank 1M HCl, while Fig. 4B showed the mild steel immersed in 1MHCl/0.9gL^{-1} *COL*. In the blank solution, coarse and uneven surface fractions were noticed with various macropores. The corrosion topography was visible enough due to the hostile nature of chloride ions in the facial dissolution layer of the steel. The micrography of mild steel in the inhibited solution (Plate 3B) differs from the control sample in 1MHCl. The level of iron

oxide formed was suppressed due to the physical form of a dense film on the facial layer of the steel. The corrosion inhibitory activity of *COL* on the mild steel surface was highly dependent on the concentration of the inhibitor.

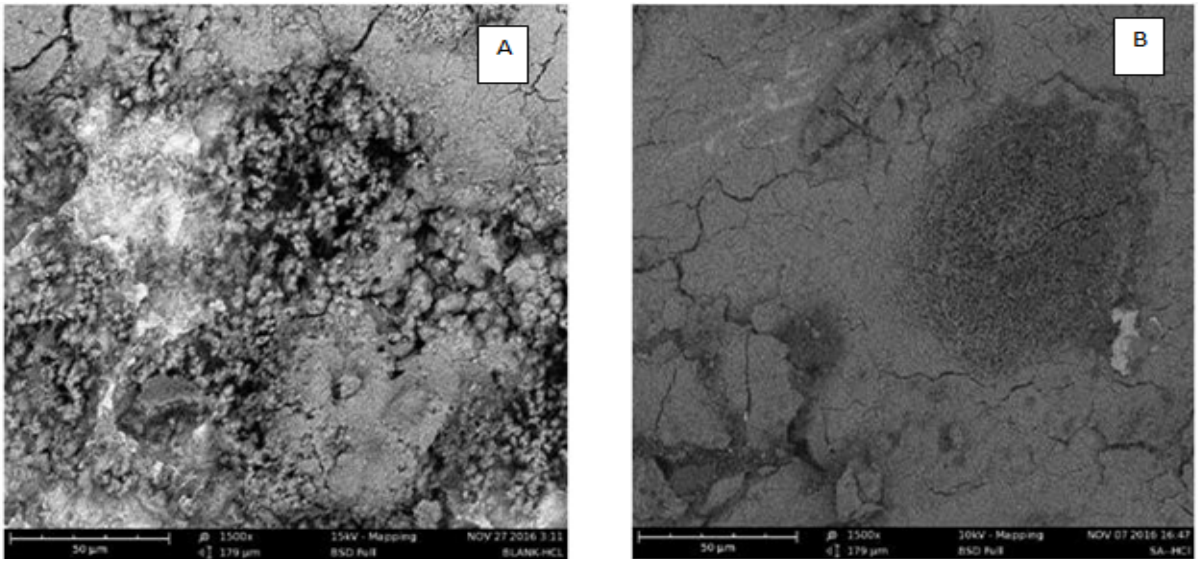

Plates 3A and 3B: SEM characteristics of the corroded mild steel in; (3A) the blank solution of 1M HCl (3B) in the presence of *CO L extract* at 0.9g per litre of 1M HCl

3.5 Potentiodynamic Polarization Analysis

Polarization experiments are carried out potentio-dynamically in unstirred 1M HCl solution in the absence and presence of a different concentration of *COL* The electrochemical parameters namely, corrosion potential (E_{corr}), corrosion current density (I_{corr}), anodic Tafel slope (b_a), cathodic Tafel slope (b_c), and percentage inhibition efficiency (IE), determined are summarized in Table 6.

Results of the potentio-dynamic polarization study, the existence of *COL* in the test solution pushed the anodic and cathodic sides to the minimum current values. The *COL* extract obstructed the anodic and cathodic sites from further reactions. The electrochemical variables, namely corrosion potential E_{corr}, and corrosion current densities $score_r$ generated from this experiment are listed in Table VI. The immersion of *COL* in HCL gently pushed E_{corr} to the anodic direction compared to the unprotected medium, while in 1M HCl the shifting mechanism in E_{corr} was not pronounced. The inconsistency in b_a and b_c values in the HCL environment decreased slightly upon the immersion of *COL* extract, which indicated corrosion inhibition promotion. The phenomenon of inhibition is due to synergistic action. In general, in a situation where the shift in E_{corr} is above 85 mV, the inhibitor can be categorized in the rank of anodic or cathodic and if the shift is lower than 85 mV the inhibitor may be seen as a mixed-type inhibitor. The results of this study revealed that the phenomenon of the inhibition is a mixed-type corrosion control, with inhibition of both cathodic and anodic reactions. Also, at elevated voltages greater than 350 mV, it was observed that metal dissolution was greater than *COL* adsorption. It could be seen from Table 6, that the corrosion current density (I_{corr}) decreased noticeably with an increase in *COL* concentration, and also the corrosion potential (E_{corr}) of mild steel shifted toward the less negative direction which suggested that *COL* behaved in a good corrosion inhibitor for mild steel in 1 M HCl solution. An inhibitor is classified as an anodic or cathodic type when the change in Ecorr value is larger than 85 mV. It is clear from table 6, that the value of Rp increased with the increasing concentration of inhibitor. The increase in Rp values was attributed to the formation of insulating protective film at the metal/solution interface.

Table 6: Electrochemical polarization parameters for Mild steel in 1M HCl solution in the absence and presence of various concentrations of *COL* extract.

Conc (%)	Tafel polarization parameters					Linear polarization Resistance parameters	
	-EcorrmV/SCE	Icorr μA/cm^2	Ba mV/dec	Bc mV/dec	IE (%)	Rohm/cm^2	IE (%)
Blank	416	1004	92	170	-	17.20	-
0.1	432	733	104	135	26.20	20.40	14.20
0.2	424	642	111	88	34.22	22.9o	23.45
0.3	493	412	100	188	57.92	30.10	41.52
0.4	431	401	79	89	60.18	52.50	66.05
0.5	462	365	128	138	62.35	62.60	71.36
0.6	471	223	73	209	76.64	68.60	73.77
0.7	431	166	70	89	78.97	99.00	81.60

3.6 Response Surface Methodology (RSM) Results

RSM results are shown in Table 7. The interactive effects of inhibitor concentration (0.5 – 0.9g/L), temperature (303 -323K) and time (1-5hrs) on the IE showed that the highest value of IE obtained was (83.33%) at the midpoint of the considered factors. This observation suggested that the relationship between IE and the considered corrosion factors of inhibitor concentration, temperature and time was parabolic.

Table 7: RSM results

Std	Run	Factor 1 An Inhibitor conc. g/L	Factor 2 B Temperature K	Factor 3 C Time hr	Response Inhibition efficiency %
5	1	0.5	303	5	57.08
4	2	0.9	323	1	51.80
14	3	0.7	313	5	78.95
3	4	0.5	323	1	47.51
13	5	0.7	313	1	65.13
7	6	0.5	323	5	48.14
8	7	0.9	323	5	61.24
10	8	0.9	313	3	79.54
17	9	0.7	313	3	83.33
12	10	0.7	323	3	68.12
19	11	0.7	313	3	83.33
11	12	0.7	303	3	77.25
20	13	0.7	313	3	83.33
1	14	0.5	303	1	52.11
2	15	0.9	303	1	58.82
6	16	0.9	303	5	70.85
9	17	0.5	313	3	75.5
16	18	0.7	313	3	83.33
15	19	0.7	313	3	83.33
18	20	0.7	313	3	83.33

3.7 Analysis of Variance (ANOVA) for the inhibition efficiency

Table 8: ANOVA for Quadratic model

Source	Sum of Squares	Df	Mean Square	F-value	p-value	
Model	3315.33	9	368.37	111.21	< 0.0001	Significant
A-Inhibitor concentration	175.64	1	175.64	53.02	< 0.0001	
B-Temperature	154.45	1	154.45	46.63	< 0.0001	
C-Time	167.20	1	167.20	50.47	< 0.0001	
AB	1.19	1	1.19	0.3603	0.5617	
AC	31.48	1	31.48	9.50	0.0116	
BC	6.00	1	6.00	1.81	0.2080	
A^2	88.71	1	88.71	26.78	0.0004	
B^2	304.03	1	304.03	91.78	< 0.0001	
C^2	342.47	1	342.47	103.39	< 0.0001	
Residual	33.13	10	3.31			
Lack of Fit	33.13	5	6.63			
Pure Error	0.0000	5	0.0000			
Cor Total	3348.46	19				
Std. Dev.	1.82		R^2		0.9901	
Mean	69.60		Adjusted R^2		0.9812	
C.V. %	2.61		Predicted R^2		0.9215	
			Model Precision		28.2273	

3.8 Mathematical Model

The mathematical model of the efficiency of the *COL* extract as a function of the considered factors is expressed in terms of coded and actual factors. A quadratic model described the systematic connections between the inhibition efficiency and the factors of, inhibitor concentration (IC), temperature (T), and time (t). The coded factors were used to evaluate the response for given levels of each factor. The coded equation is useful in determining the impact of the factors. The analysis of variance (ANOVA) is presented in Table 8. The model F-value of 111.21 implies that the model is significant and the *COL* concentration dominated in this study, followed by time and temperature, respectively. There is only a 0.01 % chance that the F-value is large due to system agitation (noise). The noise may be assigned to the flow rates of the bioactive constituents present in the *COL* extract. Values of 'Prob>F' lower than 0.0500 indicate model terms are significant. Here A, B, C, AB, AC, BC, and A^2 are significant model terms. Values higher than 0.1000 indicate the model terms are not significant. The 'Pred R-squared' of 0.9901 conforms strongly with the 'Adj R-squared' of 0.9812, and the variation is lower than 0.2. The coefficient of determination, R^2, depicts good statistical agreement between the observed and predicted values. 'Adeq. precision' evaluates the signal to noise ratio. A ratio above 4 is adequately acceptable. The ratio of 28.23 indicates a good signal. This model can be used to navigate the design space. Accordingly, the quadratic regression model is adequate for predicting the inhibition efficiency of the *COL* extract (Ernest et al., 2019; Ezeh & Onukwuli, 2021)

Final Equation in Terms of Coded Factors

$$\text{Inhibition efficiency} = +83.28 + 4.19A - 3.93B + 4.09C - 0.3863AB + 1.98AC - 0.8663BC - 5.68A^2 - 10.51B^2 - 11.16C^2 \quad (5.1)$$

$$\text{Inhibition efficiency} = +83.28 + 4.19A - 3.93B + 4.09C + 1.98AC - 5.68A^2 - 10.51B^2 - 11.16C^2 \quad (5.2)$$

3.9 Graphical Analyses of corrosion parameters interaction

Graphical analyses of the inhibition efficiency of the inhibitor for the corrosion control of mild steel in HCl are shown in Figures 2-5. In Figure 2 plot of predicted versus actual inhibition efficiency showed a linear graph. It is a linear graph. The points clustered along the line of best fit. It revealed that the generated model can adequately describe the efficiency of the corrosion control process. Figures III-V show 3-dimensional (3-D) plots of the interactive effects of the inhibitor concentration, temperature, and time on the inhibition efficiency. The graphs showed parabolic curves with optimum inhibition efficiency of 83.33%.

The inhibition efficiency increased with an increase in *COL* concentration until it reached the optimum point. The increase in the *COL* concentration expedited the formation of a dense film layer in the physical state. However, the efficiency declined with an increase in temperature, because an increase in temperature disorganizes the heterocyclic bonds of the extract. The temperature rise reduces the adsorption activity on the metal surface, especially when the mutual correlation between the metal and the inhibitor is quite low. Fig. 3 shows the interactive effect of temperature and inhibitor concentration on the efficiency of the *COL*.

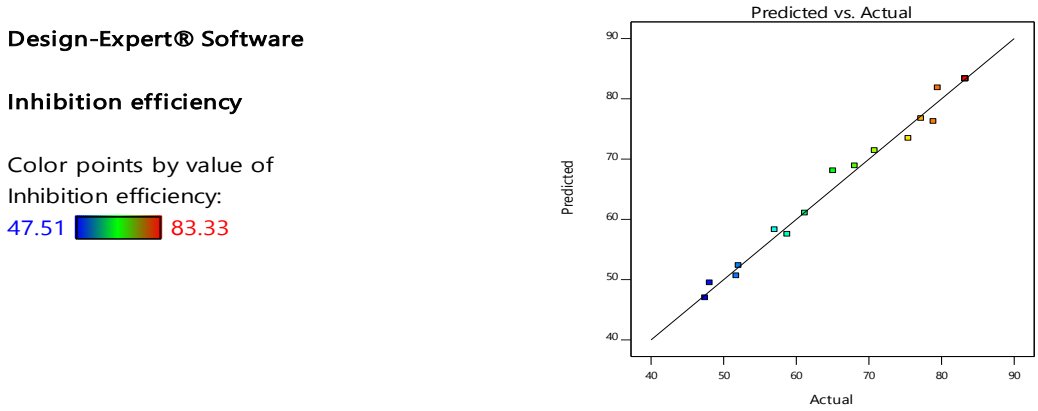

Figure 2: Predicted versus actual plot

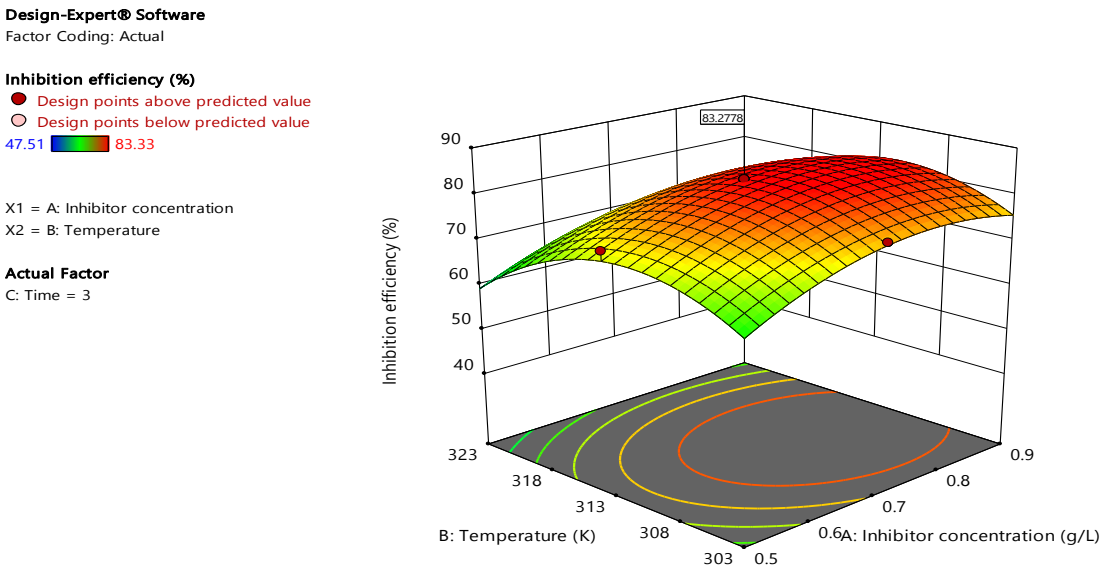

Figure 3: Inhibition efficiency versus inhibitor concentration and temperature

An increase in the inhibitor concentration reduces the corrosion of mild steel. This reduction may be attributed to the level of adsorption of polyphenols and heteroatoms of the *COL* molecules which block the active sites of the steel surface from further activity, thereby giving an efficiency of 83.30 %. Figures 3 and 5 showed the negative influence of temperature on corrosion rate. Increasing this variable reduces

the corrosion inhibition efficiency of *COL* extract. It created local anodes and cathodes on the surface, which increased the corrosion rate.

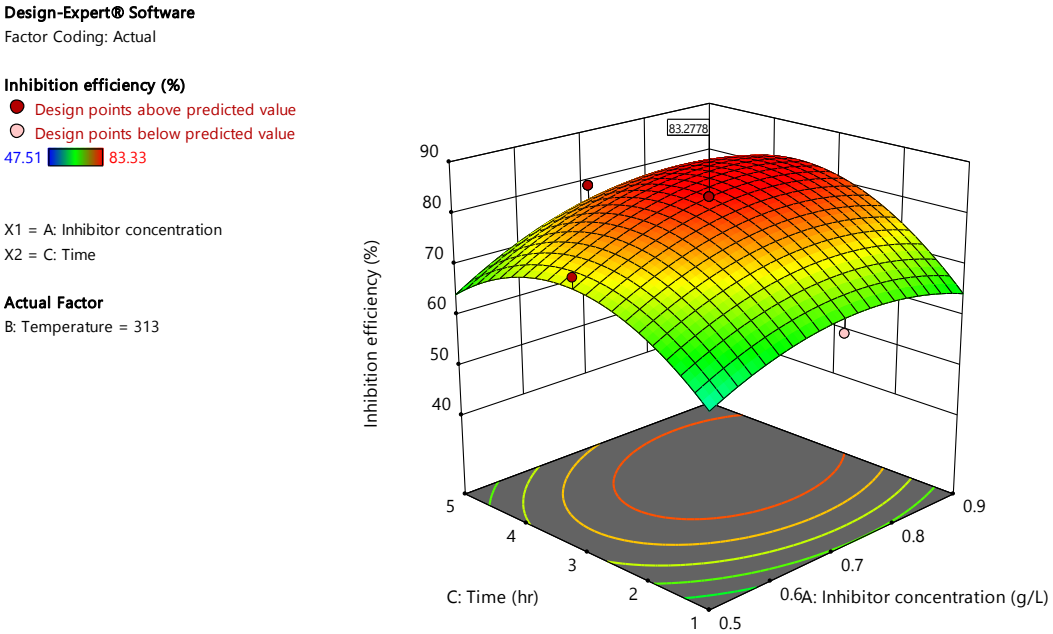

Figure 4: Inhibition efficiency versus inhibitor concentration and time

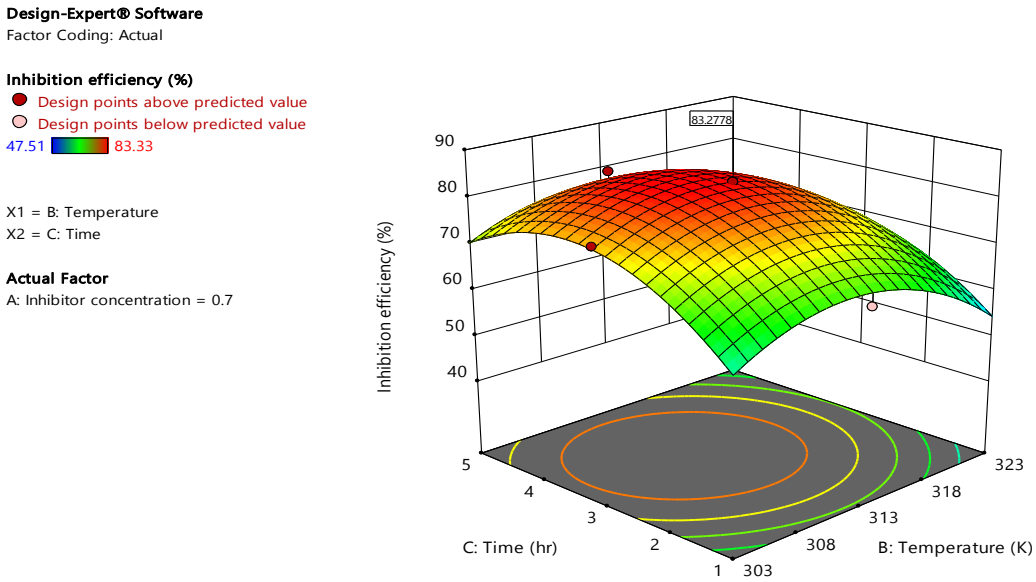

Figure 5: Inhibition efficiency versus temperature and time

4. Validation of the Optimum Parameters

To confirm the validity of the results, an additional experiment was conducted. As shown in Table 9, the value of experimental inhibition efficiency (83.42%) was close to the predicted value (83.33%). The percentage deviation of 2.19% is less than 5%. It showed that the generated models adequately predicted the inhibition efficiency of *COL* extract.

Table 9: Validation of the result

Inhibitor conc. (g/L)	Temp. (K)	Time (hr)	Predicted IE (%)	Experimental IE (%)	Percentage Deviation (%)
0.7	313	3	83.33	85.2	2.19

Conclusions

it was found from the tests conducted that the *COL* plant extract used exhibited good corrosion inhibition with mild steel corrosion in a 1M HCl environment. The inhibition efficiency of *COL* plant extracts increased with the increasing concentration of the active material. The addition of low concentrations of the inhibitor to the system studied led to a significant decrease in the corrosion rate. This proves that the use of pure green inhibitors reduces the corrosion rate in the 1M HCl corrosive media and that the inhibition efficiency of the tested natural inhibitor is promising. Electrochemical analysis showed that the *COL* natural inhibitor used was a mixed-type inhibitor. The charge transfer resistance increased with an increase in inhibitor concentration. The decrease in charge density as the concentration of the inhibitor increased indicated that the corrosion rate is reduced as the inhibition efficiency of the inhibitor increases. These findings are worth comparing with the availability, performance, cost, and environmental impact of the widely used synthetic and commercially applied corrosion inhibitors. It is also worth investigating the impact of formulating mixtures of green corrosion with some coactive, synergizes, surfactants, and indifferent solvents to serve a wide range of industrial applications.

Declarations

Ethics approval
Not applicable
Consent to participate
Not applicable
Availability of data and material
Not applicable
Competing interest
The authors declare no conflict of interest.
Code availability
Not applicable
Funding
The authors received no funding for this study
Consent for publication
Not applicable
Authors contributions : Dr Ezeh E M conceived and initiated the research work. Agu P C sourced the literature and rectified the article.

References

Aniobi C. C., Okeke O., Ezeh, E., Okeke, H. C., & Nwanya, K. O. (2021). Comparative Assessment of the Phytochemical and Selected Heavy Metal Levels in <i>Cucumis sativus</i> L. and <i>Solanum aethiopicum</i> L. Fruit Sample Grown in South Eastern and North Central Regions of Nigeria Respectively. *Natural Resources*, *12*(08). https://doi.org/10.4236/nr.2021.128016

Aoufir E.Y., Bakri Y. El, Kerroum Y., Lgaz H., Harmaoui A., Chetouani A., Sebhaoui J., Salghi R., Ramli Y., Guenbour A., Essassi E. M., Oudda H. (2017). Triazole derivative as new and effective corrosion inhibitor for carbon steel in hydrochloric acid: Electrochemical and quantum chemical studies. *Mor. J. Chem.* 5, 545-559. doi.org/10.48317/IMIST.PRSM/morjchem-v5i4.8979

Ashmawy, A. M., & Mostfa, M. A. (2021). Study of eco-friendly corrosion inhibition for mild steel in acidic environment. *Egyp. J. Chem.*, *64*(3). doi.org/10.21608/EJCHEM.2020.39538.2806

Begum, A. A. S., Vahith, R. M. A., Kotra, V., Shaik, M. R., Abdelgawad, A., Awwad, E. M., & Khan, M. (2021). Spilanthes acmella leaves extract for corrosion inhibition in acid medium. *Coatings*,

11(1). https://doi.org/10.3390/coatings11010106
Bouayad K., Kandri Rodi Y., El Ghadraoui E. H., Elmsellem H., Ouzidan Y., El Mahi B., Essassi E. M., Abdel-Rahman I., Chetouani A., & Hammouti B. (2017). Corrosion Protection of Mild Steel in Hydrochloric Acid at 308 K using Benzimidazole Derivatives: Weight Loss, Adsorption and Quantum Chemical Studies. *Mor. J. Chem.* 5(2), 22-34 https://doi.org/10.48317/IMIST.PRSM/morjchem-v6i1.9735
Denissen, P. J., & Garcia, S. J. (2019). Reducing subjectivity in EIS interpretation of corrosion and corrosion inhibition processes by in-situ optical analysis. *Electrochimica Acta*, *293*. https://doi.org/10.1016/j.electacta.2018.10.018
Edoziuno F. O., Adediran, A. A., Odoni, B. U., Akinwekomi, A. D., Adesina, O. S., & Oki, M. (2020). Optimization and development of predictive models for the corrosion inhibition of mild steel in sulphuric acid by methyl-5-benzoyl-2-benzimidazole carbamate (mebendazole). *Cogent Engineering*, *7*(1). https://doi.org/10.1080/23311916.2020.1714100
Ernest E., Onyeka, O., C. M., A., C. C., A., & J. O, N. (2019). Adsorption Efficiency of Activated Carbon Produced from Corn Cob for the Removal of Cadmium Ions from Aqueous Solution. *Academic Journal of Chemistry*, *44*. https://doi.org/10.32861//ajc.44.12.20
Ezeh E. M., & Onukwuli, O. D. (2020). Physicochemical characterization of cow horn ash and its effect as filler material on the mechanical property of polyester-banana fibre composite. *World Journal of Engineering*, *17*(6). https://doi.org/10.1108/WJE-08-2020-0351
Ezeh E. M., & Onukwuli, O. D. (2021). Comparative Cone calorimetric analysis of the fire retardant properties of natural and synthetic additives in banana peduncle fibre reinforced polyester composites. *Mor. J. Chem.*, *9*(3), 530-541. https://doi.org/10.48317/IMIST.PRSM/morjchem-v9i3.21954
Ezeh E. M., Onukwuli, O. D., & Odera, R. S. (2019). Novel flame-retarded polyester composites using cow horn ash particles. *International Journal of Advanced Manufacturing Technology*, *103*(5–8). https://doi.org/10.1007/s00170-019-03678-2
Farssi M., Batah A., Belkhouda M., Salghi R., Gharby S., Mamouni R., Laknifli A., Bammou L. (2020). Green inhibition of carbon steel corrosion by fish oil in hydrochloric acid medium. *Mor. J. Chem.*, 8, 474-485. https://doi.org/10.48317/IMIST.PRSM/morjchem-v8i2.18592
Fateh A., Aliofkhazraei, M., & Rezvanian, A. R. (2020). Review of corrosive environments for copper and its corrosion inhibitors. *Arabian Journal of Chemistry,* 13(1). https://doi.org/10.1016/j.arabjc.2017.05.021
Guo W., Umar, A., Zhao, Q., Alsaiari, M. A., Al-Hadeethi, Y., Wang, L., & Pei, M. (2020). Corrosion inhibition of carbon steel by three kinds of expired cephalosporins in 0.1 M H_2SO_4. *Journal of Molecular Liquids*, *320*. https://doi.org/10.1016/j.molliq.2020.114295
Guruprasad A. M., Sachin, H. P., Swetha, G. A., & Prasanna, B. M. (2020). Corrosion inhibition of zinc in 0.1 M hydrochloric acid medium with clotrimazole: Experimental, theoretical and quantum studies. *Surfaces and Interfaces*, *19*. https://doi.org/10.1016/j.surfin.2020.100478
Hashim N. Z. N., Anouar, E. H., Kassim, K., Zaki, H. M., Alharthi, A. I., & Embong, Z. (2019). XPS and DFT investigations of corrosion inhibition of substituted benzylidene Schiff bases on mild steel in hydrochloric acid. *Applied Surface Science*, 476. https://doi.org/10.1016/j.apsusc.2019.01.149
Jing C., Dong, B., Raza, A., Zhang, T., & Zhang, Y. (2021). Corrosion inhibition of layered double hydroxides for metal-based systems. *Nano Materials Science*, *3*(1). https://doi.org/10.1016/j.nanoms.2020.12.001
Lou Y., Chang, W., Cui, T., Wang, J., Qian, H., Ma, L., Hao, X., & Zhang, D. (2021). Microbiologically influenced corrosion inhibition mechanisms in corrosion protection: A review. *Bioelectrochemistry*, *141*. https://doi.org/10.1016/j.bioelechem.2021.107883
Mechbal N., Mechbal, N., Karzazi, Y., Abrigach, F., El-Hajjaji, F., & Hammouti, B. (2016). Experimental study of the corrosion inhibition of mild steel by the N1, N1, N5, N5-tetrakis ((1H-pyrazol-1-yl) methyl) naphthalene-1,5-diamine in hydrochloric acid solution. *Mor. J.*

Chem., 4, 876-890. https://doi.org/10.48317/IMIST.PRSM/morjchem-v4i4.7219
O.D, O., & Ezeh, E. M. (2021). Assessment of the fire retardant effect potential of carbonized cow horn ash additive in banana peduncle fibre reinforced polyester composites. *World Journal of Engineering*. https://doi.org/10.1108/WJE-07-2021-0438
Ogunleye O. O., Arinkoola, A. O., Eletta, O. A., Agbede, O. O., Osho, Y. A., Morakinyo, A. F., & Hamed, J. O. (2020). Green corrosion inhibition and adsorption characteristics of Luffa cylindrica leaf extract on mild steel in hydrochloric acid environment. *Heliyon*, 6(1). https://doi.org/10.1016/j.heliyon.2020.e03205
Onyeka O., Ifeyinwa, O. C., Ernest, E., Adunola, I. B., & Onyinye, N. J. (2020). Out-Door Air Pollution Levels in Vehicular-Traffic Junctions in Nsukka Metropolis, Enugu Metropolis and Awgu Semi-Urban Area in Enugu State, Nigeria. *Open Journal of Air Pollution*, *09*(04). https://doi.org/10.4236/ojap.2020.94007
Rocca E., Faiz, H., Dillmann, P., Neff, D., & Mirambet, F. (2019). Electrochemical behavior of thick rust layers on steel artefact: Mechanism of corrosion inhibition. *Electrochimica Acta*, *316*. https://doi.org/10.1016/j.electacta.2019.05.107
Rostampour B., Seifzadeh D., Abedi, M., & Shamkhali, A. N. (2020). Synthesis and Characterization of a New N4S2 Schiff base and Investigation of its Adsorption and Corrosion Inhibition Effect by Experimental and Theoretical Methods. *Protection of Metals and Physical Chemistry of Surfaces*, *56*(1). https://doi.org/10.1134/S2070205120010189
Sabbahi M., El Hassouni A., Tahani A., & El Bachiri A. (2020). Altitude effect on the chemical composition and antioxidant activity of rosemary in the region of Talsint (Morocco). *Mor. J. Chem.*, 8, 866-875. https://doi.org/10.48317/IMIST.PRSM/morjchem-v8i4.18311
Song D., Yu, W., & Yang, H. (2021). Scale and corrosion inhibition performance of carboxymethyl chitosan. *Scientia Sinica Chimica*, *51*(5). https://doi.org/10.1360/SSC-2020-0220
Sulaiman K. O., Onawole, A. T., Faye, O., & Shuaib, D. T. (2019). Understanding the corrosion inhibition of mild steel by selected green compounds using chemical quantum based assessments and molecular dynamics simulations. *Journal of Molecular Liquids*, *279*. https://doi.org/10.1016/j.molliq.2019.01.136
Umoren S. A., Eduok, U. M., Solomon, M. M., & Udoh, A. P. (2016). Corrosion inhibition by leaves and stem extracts of Sida acuta for mild steel in 1 M H2SO4 solutions investigated by chemical and spectroscopic techniques. *Arabian Journal of Chemistry*, *9*. https://doi.org/10.1016/j.arabjc.2011.03.008
Wood M. H., & Clarke, S. M. (2017). Neutron reflectometry for studying corrosion and corrosion inhibition. In *Metals* (Vol. 7, Issue 8). https://doi.org/10.3390/met7080304
Yan Y., Shi, H., Wang, J., Liu, F., & Han, E. H. (2019). Corrosion Inhibition of Galvanized Steel in NaCl Solution by Tolytriazole. *Acta Metallurgica Sinica (English Letters)*, *32*(4). https://doi.org/10.1007/s40195-018-0777-6
Zheng Y. X., Wang, X. P., & Zong, L. N. (2021). Advance on natural polysaccharides and its derivatives in metal corrosion inhibition. *Surface Technology*, *50*(2). https://doi.org/10.16490/j.cnki.issn.1001-3660.2021.02.022
Zinad D. S., Jawad, Q. A., Hussain, M. A. M., Mahal, A., Mohamed, L., & Al-Amiery, A. A. (2020). Adsorption, temperature and corrosion inhibition studies of a coumarin derivatives corrosion inhibitor for mild steel in acidic medium: Gravimetric and theoretical investigations. *International Journal of Corrosion and Scale Inhibition*, *9*(1), 134-151. https://doi.org/10.17675/2305-6894-2020-9-1-8